Volume 45 http://acousticalsociety.org/

181st Meeting of the Acoustical Society of America

Seattle, Washington

29 November - 3 December 2021

Underwater Acoustics: Paper 2aCA10

Design of an underwater acoustics lab

Cameron T. Vongsawad, Tracianne B. Neilsen, Adam D. Kingsley, John E. Ellsworth, Brian E. Anderson, Kaylyn N. Terry, Corey E. Dobbs, Scott E. Hollingsworth and Gabriel H. Fronk

Department of Physics and Astronomy, Brigham Young University, Provo, UT, 84602; cvongsawad@gmail.com; tbn@byu.edu;tbnbyu@gmail.com; adamkingsley@gmail.com, jee@byu.edu, bea@byu.edu, knterry@gmail.com, coreydobbs205@gmail.com, scottphollingsworth@gmail.com, gherrickfronk@gmail.com

A new underwater acoustics laboratory has been created at Brigham Young University. Care was taken to design the lab that can take high precision measurements and yet provide an optimal environment for training undergraduate student researchers. The laboratory water tank is a rectangular acrylic tank of 3.6 m long by 1.2 m wide with 0.91 m as the maximum depth. This paper provides details about the custom-built water treatment and sanitizer with bubble removal column. The measurement chain for signal transmission and recording and the automated positioning system are explained. Sound absorbing tiles acquired to line the side walls are also described. The *in situ* calibration method for obtaining a through-the-sensor frequency response of the entire measurement chain is presented. Limitations are mentioned along with a discussion of how this design maintains potential for a wide variety of underwater acoustic laboratory measurements.

Published by the Acoustical Society of America

 https://doi.org/10.1121/2.0001540

1. INTRODUCTION

The Underwater Acoustics Laboratory at Brigham Young University (BYU) was designed and constructed during the years 2019-2021 to facilitate high quality research. Because of the priority on mentored undergraduate student research at BYU, each component was selected with considerations for high levels of safety, automation, and reliability. These features give students the opportunity to learn to perform effective acoustical measurements and data analysis in a mentored environment. More about the mentored environment can be found in the paper Vongsawad, *et al.*[1] submitted to The Journal of the Acoustical Society of America's Special Issue on Education in Acoustics. That paper focuses on mentoring and does not go into the details about the measurement system; the purpose of the current proceedings paper is to provide those details and a description of the through-the-sensor calibration process.

In addition to providing opportunities to train students, this lab provides a way to test algorithms that can be applied to open-water data. Obtaining large open-water data sets for underwater acoustics research and validating measurements[2–4] has high economic and temporal costs. A laboratory system saves on those costs,[5] especially for researchers without ease of access to large bodies of water.[6,7] Open-water tests are often noisy and unpredictable with ever changing environmental concerns, but the tank allows for better control of the environment.[7] Measurement automation allows data to be collected quickly and efficiently, with high precision.

This paper provides details about the water tank, water treatment and sanitizer system, anechoic panels, signal transmission and data acquisition, and the automated positioning system. The *in situ* calibration method for obtaining a through-the-sensor frequency response of the entire measurement chain is also presented. In conclusion, a few limitations of this experimental setup are mentioned along with a discussion of how this design maintains potential for a wide variety of underwater acoustic laboratory measurements.

2. EXPERIMENTAL SETUP

The open-air rectangular parallelepiped water tank, shown in Fig. 1, was made by Engineering Laboratory Design Inc. (Lake City, Minnesota, USA) and is constructed of scratch resistance acrylic panels that are solvent-welded together, with a steel frame on adjustable leveling pads. The tank material, acrylic, was also chosen for its visual transparency and non-corrosive nature. Acoustical reflections from these walls are reduced compared to tanks made of steel, concrete, or glass since the acoustic impedance of acrylic is closer to that of water than those other materials.[5] (Values for lucite are found in Kinsler & Frey on p. 256.) The tank's dimensions were chosen to allow scaled acoustical measurements, similar to work in Refs. [3–5,8–10] and designed to maximize usable laboratory space. The 3.66 m long by 1.22 m wide rectangular tank has a maximum water depth of 0.91 m, corresponding to a maximum fill volume of 4077.6 liters.

A. WATER TREATMENT

Water quality is maintained by a system that provides for filtration, sanitization, temperature control, and bubble reduction. Acoustic disturbances caused by thru wall plumbing penetrations of the tank are avoided by siphoning water out of the tank over the wall and returning it after treatment over the wall. The pickup (inlet) and return (outlet) siphon pipes are removable so the filtration system can be separated from the tank entirely. Bubble prevention is accomplished by exposing water returning to the tank to a low pressure in the vertical column. Dissolved air and small bubbles expand and float to the top of the column and are removed. Control of pumps, valves, and heating is automated using a programmable logic controller (PLC). A piping diagram of the system is shown in Fig. 2a with water components depicted in blue and air control components in green. Water flow in the diagram is left to right. A photo of the treatment system is provided in Fig. 2b with letters indicating the different parts. The system incorporates a water pump (W), a micron

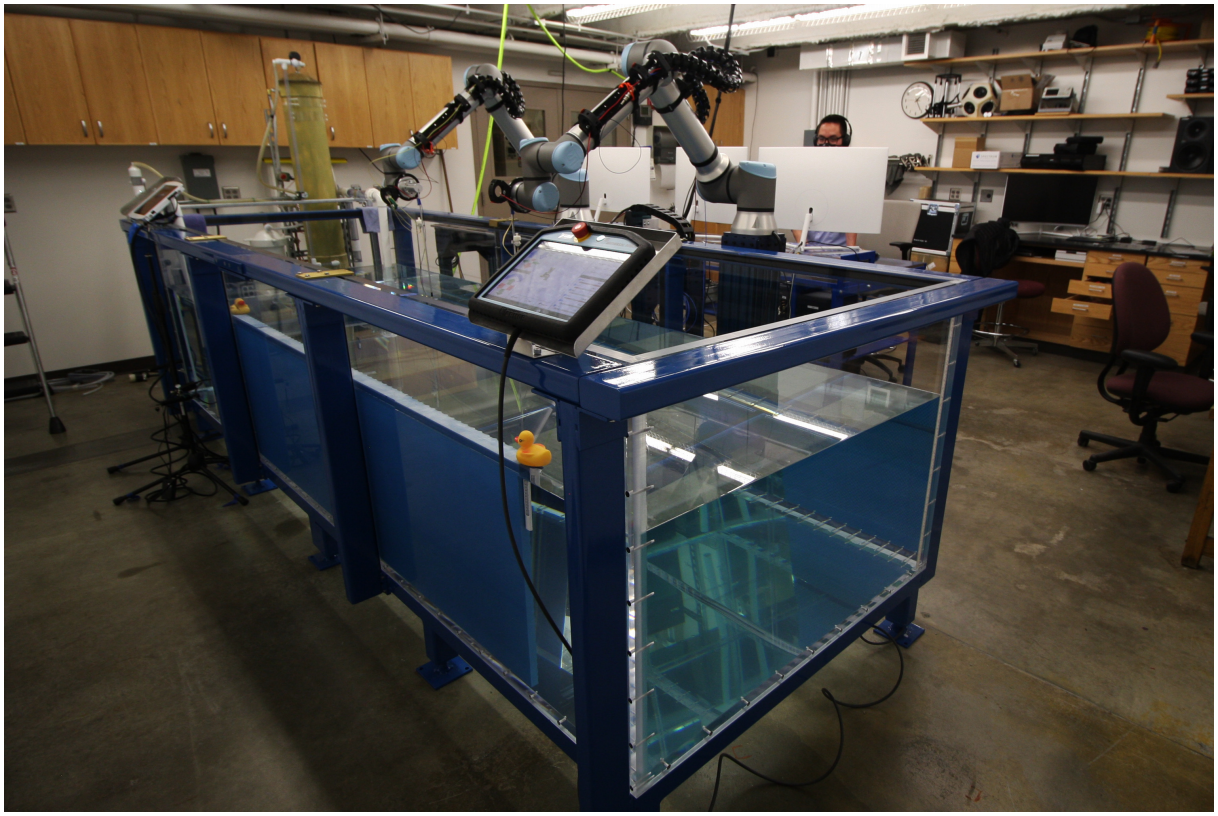

Figure 1: BYU's acrylic water tank and robotic positioning system.

bag filter (Q), a water heater, an ultraviolet light water sanitizer, an ozone generator (behind the controls cabinet V). Bubble prevention is provided by a vacuum pump (J) that removes air from all components of the water path using three solenoid valves (G and M), three manual flow rate valves (H), a check valve (I), and drain line (K). Three vent valves are provided for inputting air where needed to adjust water levels (F). Four capacitance water level detectors are used, one on each of the inlet (U) and outlet (E) sight glasses and two (C and D) on the bubble removal column (B). Temperature is monitored by a J-type thermocouple probe (S) positioned at the water inlet. Pipe unions for connecting and removing the siphon inlet (O) and return pipe are installed to be close to the tank. A sight glass (L) and a compound pressure gauge (A) are used for setting up water levels when installing the filtration system. The pressure gauge (N) is used to monitor the condition of the filter. The electronics, PLC, and control display panel (R) are housed in a watertight cabinet (V). The system is powered by three-phase 208 AC and equipped with a ground fault interrupter (T). A requisite emergency stop button (P) is provided above the control system.

To allow ease of both draining and filling, a valve is located in one corner of the bottom sheet of acrylic, with a direct line split to either a drain or water faucet. The valve can be capped with a flat acrylic insert to eliminate unnecessary scattering. The insert has an embedded iron piece for easy removal with a magnet. Tap water is used to fill the tank, with the water level replenished using distilled water as gradual evaporation occurs in order to maintain control over the water properties and thus the speed of sound. Distilled water replaces the evaporated water without introducing increased calcium hardness or other changes to water properties. Since distilled water is mineral depleted, the tank is never filled entirely with distilled water which is highly corrosive, especially to metals such as those associated with the body of some underwater transducers and the transducer mounts.

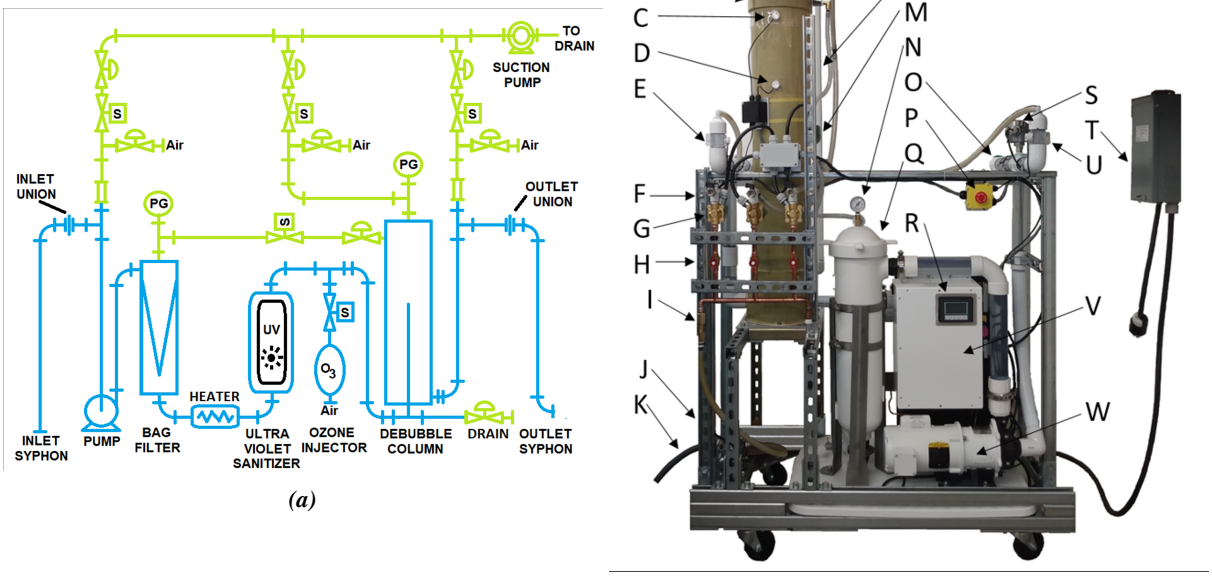

(a) *(b)*

Figure 2: (a) Piping and instrument diagram of the filter and sanitation system with water control components in blue and air control components in green. (b) Water filtration and sanitation engine, front view. See text for a description of the components corresponding with the alphabetic labels.

B. ABSORPTIVE PANELS

To reduce the reflections from the side walls, panels of attenuating material (polyurethane) are used. The attenuating material from Precision Acoustics was chosen to reduce side-wall reflections especially for ultrasonic frequencies. The 50 mm thick, 60 cm tall, square Apltile SF5048 panels, shown in Fig. 3, are optimized for 20-200 kHz and advertise an echo reduction greater than 30 dB. Initial investigations into how lining the tank walls with these panels reduces the reverberation time and the spatially averaged absorption are presented in Ch. 4 of Ref. 11.

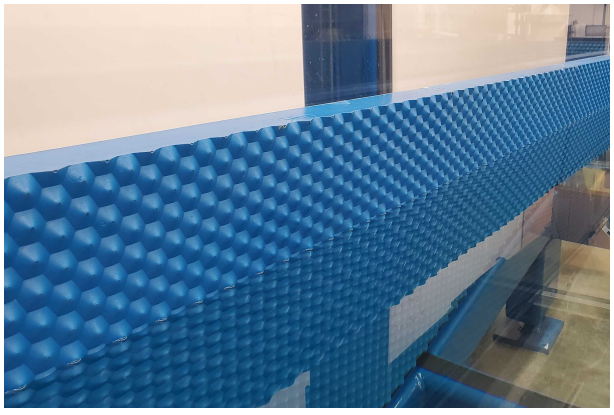

Figure 3: Apltile SF5048 anechoic panels, made by Precision Acoustics.

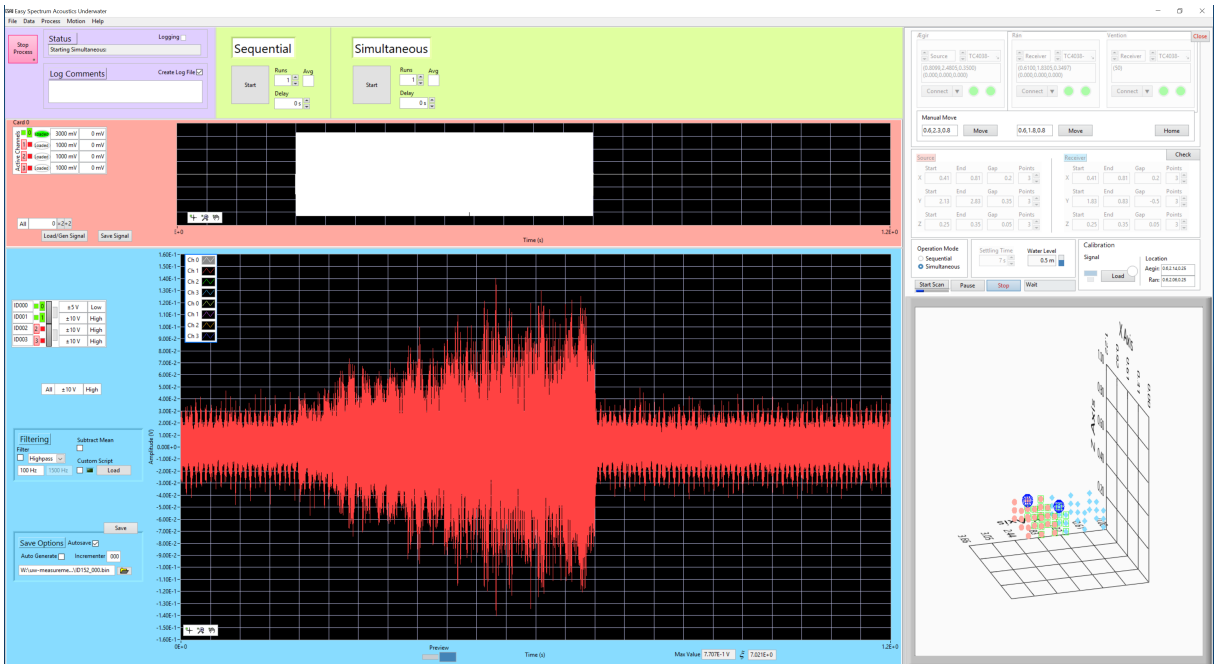

Figure 4: The ESAU interface: custom LabVIEW software used for signal generation (pink box) and data acquisition (blue box), and sensor positioning using the UR10e robotic arms (right side).

C. DATA ACQUISITION SYSTEM

Sensor positioning, signal generation, and data acquisition are controlled via custom LabVIEW software, referred to as Easy Spectrum Acoustics Underwater, or ESAU, whose interface is shown in Fig. 4. ESAU, created by author ADK, facilitates user communication with the Spectrum data acquisition cards and the UR10e robotic arms. The data acquisition cards have relatively high resolution (16-bit) and high sampling rate (40 MS/s). Using the Star-Hub module, the arbitrary waveform generator (AWG) (M2p.6546-x4) and digitizer (M2p.5932-x4) cards are accurately synchronized while housed inside an external PCIe chassis. As implemented, the shared memory allows for 128 mega samples for each of the four input and four output channels. The chassis are seen in the center of the lower shelf in Fig. 8.

D. POSITIONING SYSTEM

The three-dimensional positioning system uses two UR10e collaborative robots from Universal-Robots (universal-robots.com), with one on a Vention (vention.io) 7th axis extender track. The robots, shown in Fig. 5, were chosen for their intuitive programming language, high level of programmable safety, and 0.01 mm precision for repeatability. Each robot operates using six axes of motion and has a maximum reach of 1.3 m. Both robots are mounted level with the top of the tank: one on a simple pedestal and the other on the Vention 7th-axis extender track with a rack and pinion motor providing an additional 1.4 m reach along the length of the tank. The extender track (shown in Fig. 6) has an added positioning error of ±0.01 mm. The Universal-Robots website contains an interactive online academy which allows students to learn robot functionality, safety, and programming in a quick, simple, and thorough way.

Several sources of uncertainty arise in our positioning system. One of them is that the two robots have independent positioning systems oriented with respect to their respective bases. In selecting measurement locations, we need a single coordinate system oriented on one corner of the tank. Conversion from the robot coordinates to the tank coordinate system adds uncertainty to the UR10e 0.01 mm precision. Attachments to

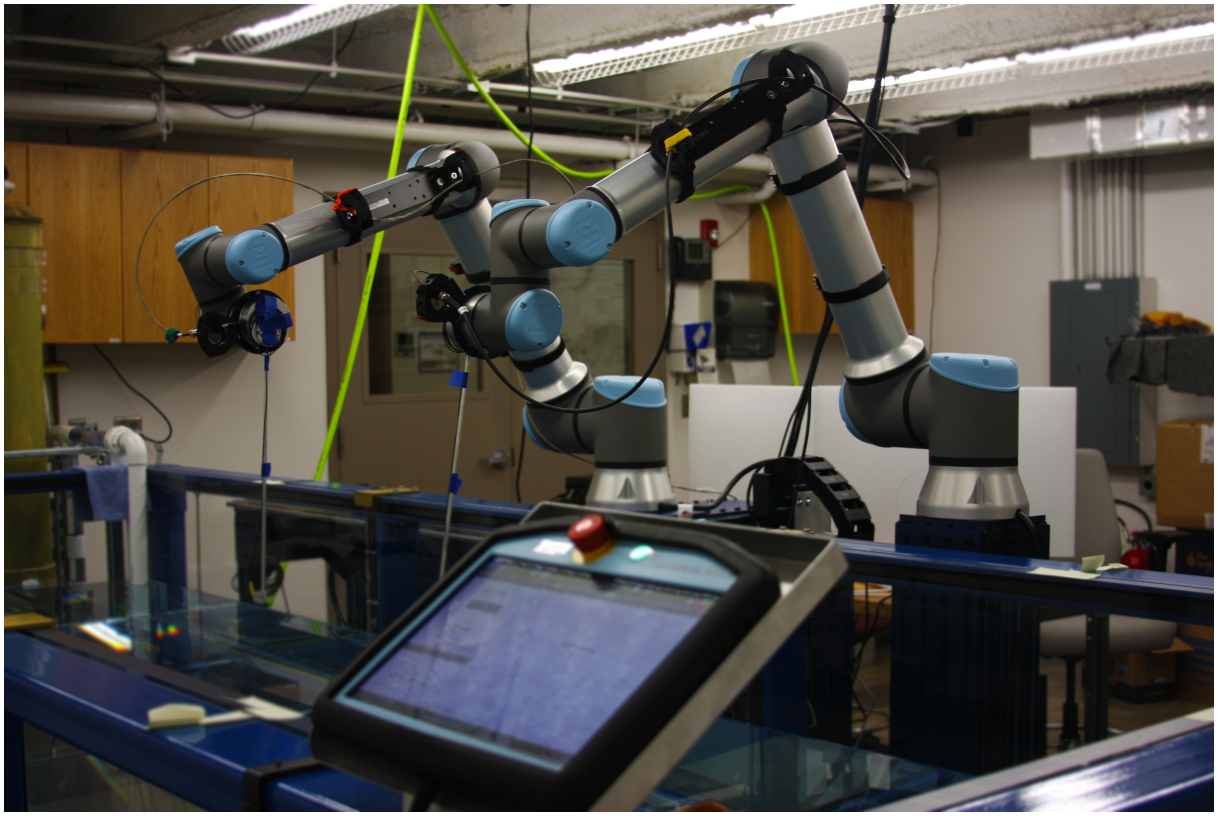

Figure 5: UR10e collaborative industrial robots for positioning sensors with teach pendant (for manual control) in the foreground.

the robotic arms also provide another source of positioning uncertainty. Because these sources of uncertainty are constant, they do not affect repeatability. For two repeated measurements, the positions are the same to ±0.01 mm. Another way this precision can be achieved is by using the distance between two positions acquired by the same robotic arm. Efforts are being made to reduce the added uncertainty in the absolute position relative to the tank coordinates as much as possible and to ensure that we properly account for the propagation of these uncertainties into measurements when necessary.

Several UR10e features are important to ensure safety, especially when new students are being trained. First, each robot has a pre-installed emergency stop button that can be pushed at any time to immediately stop and lock the robot. In addition, the robots have been wired together so that stopping one also stops the other. The desired operational range of each robot is programmed in using a teach pendant—the device used to interact directly with the robots—to define boundary planes. The robot does not exceed these boundary planes as it moves to a requested position, which is important to ensure no part of the robot hits the walls of the tank. The robots have a force tolerance that engages the brakes as well. We have added an additional safety feature to our robots to ensure that they are not accidentally moved into the water; each one has a FS25-C111 float switch from SMD Fluid Controls that will send a stop signal if the float switch touches the water. The float switch is shown in Fig. 7a approximately 7 cm below the end of the robot.

Transducers may be attached to the UR10e in any orientation via custom-designed mounts, referred to as tools. Each transducer has a custom attachment on a thin rod extended from the robot (Fig. 7a) to maintain orientation of the transducers and protect the robot from water damage. This feature allows for more flexibility than traditional two or three axis positioning systems while maintaining similar precision.[9,10]

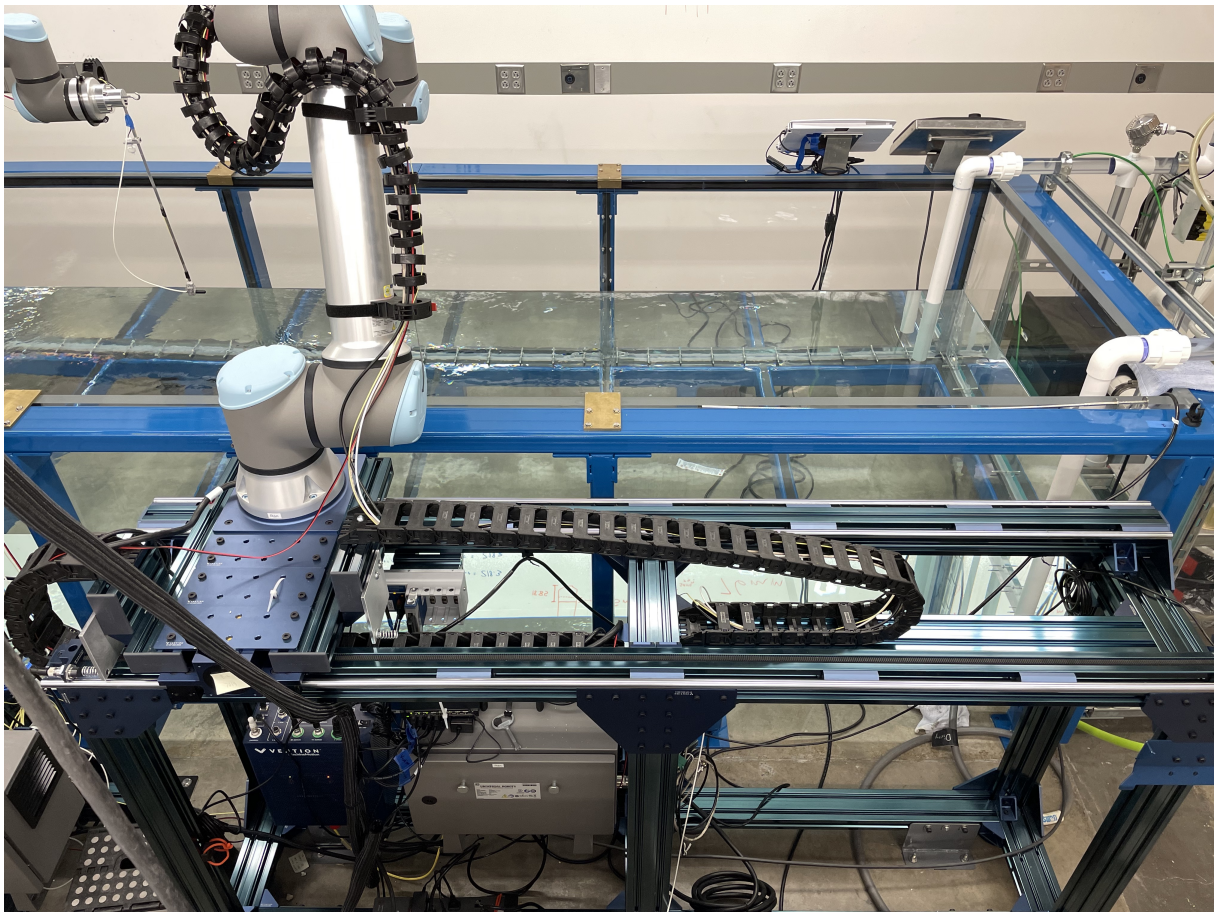

Figure 6: UR10e collaborative industrial robot on the Vention 7th axis extender

The custom transducer mounts allow for multiple configurations including an added wire PTFE/FEP Tip Probe (K-37X-T) thermocouple from ThermoWorks (shown in Fig. 7b at the end of the yellow wire) to measure temperature[2] without significant increased scattering. Conditions are also monitored with SensorsOne LMP 307T temperature and pressure/depth sensors from MCT RAM (mctram.com), rated for 0-86°F and up to 250 m depth. These sensors can be attached to the tank walls using magnets, as shown in in Fig. 7c. The output from two of these sensors are monitored continuously using an NI USB-TC01 boxes and LabVIEW software.

The automated positioning is controlled through TCP/IP by custom LabVIEW software (Fig. 4) used for the data acquisition. Users input coordinates or grids of coordinates in the LabVIEW software, ESAU; if the requested locations fit within defined safety limits, the locations are sequentially sent to the robot and a recording is made at each location. Each robot's software then interpolates between available robot arm/tool orientations to maintain consistent orientation relative to the transducer directivity.

E. MEASUREMENT CHAIN

The automated measurement system can be used with a variety of transducers for transmitting and receiving sound. The frequency range of interest is the primary factor in determining which transducers to use. Currently, we use Brüel Kjær 8103 for the 0.1 Hz - 100 kHz band and Teledyne Reson TC4038 for the 100 kHz - 500 kHz band. These sensors are used for both transmitting and receiving due to their reciprocity,

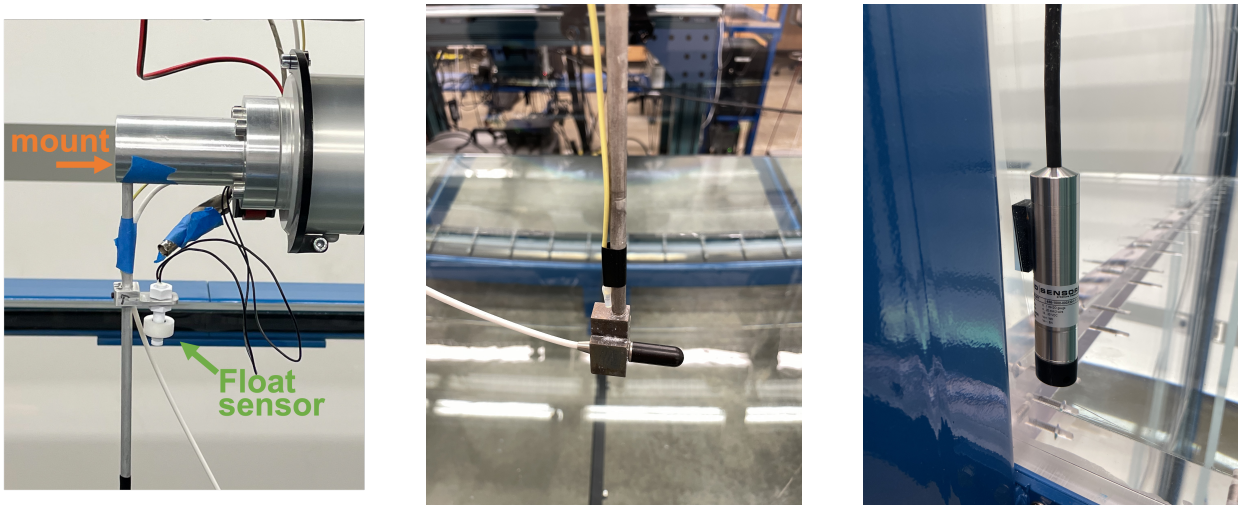

(a) *(b)* *(c)*

Figure 7: (a) Custom mount on the UR10e with a white FS25-C111 float sensor. (b) A B&K 8103 hydrophone and K-37X-T thermocouple. (c) SensorsOne LMP 307T temperature and pressure/depth sensor from MCT RAM.

omnidirectionality, and relatively flat frequency response over the specified bands.

The transmitting transducer receives the output signal from the arbitrary waveform generator (AWG) passed through a power amplifier (TEGAM Model 2350). The TEGAM allows a maximum of 4 Vpp input before clipping and provides a gain of x50. For frequencies above 10 kHz,[12] the TEGAM output is passed through a transformer fabricated to address the impedance mismatch often found between an amplifier and a piezoelectric source.[7] Two of these TEGAM power amplifiers are shown on the left side of the lower shelf in Fig. 8.

The receiving transducers are connected to a conditioner. Signals from the B&K 8103 are passed through a B&K signal conditioner. Signals from the TC4038 are passed through Teledyne Marine Reson VP2000 EC6081 mk2 preamplifiers, as described in Ref. [13]. These signal conditioners sit on the main desk in Fig. 8, under the monitors. The conditioned voltage signals are then sent to the Spectrum digitizer cards, described above.

The cables connecting transducers to the data acquisition system run along the length of the robotic arms and require special consideration of shielding to reduce the potential for induced noise from robot motors and brakes. These cables are contained in a cable management system to prevent cables from entering the water or becoming entangled. All of these cables and electrical equipment are kept on one side of the tank to provide organization and maintain a clear location for maintenance to be completed while minimizing potential water damage, as described in Appendix C of Ref. [11].

3. THROUGH-THE-SENSOR CALIBRATION

Because each component of the measurement chain has a different frequency response, a through-the-sensor calibration method is used. Using a closely spaced transmitter and receiver pair, a recorded chirp is processed via cross correlation to obtain the impulse response of the system.[14,15] The procedure used here uses techniques in room acoustics and is similar to the procedure in Ref. 16, except that they were doing source characterization and we are obtaining the frequency response of the measurement chain with minimal propagation effects.

In practice, the frequency response of the measurement chain includes the effects of the response of the

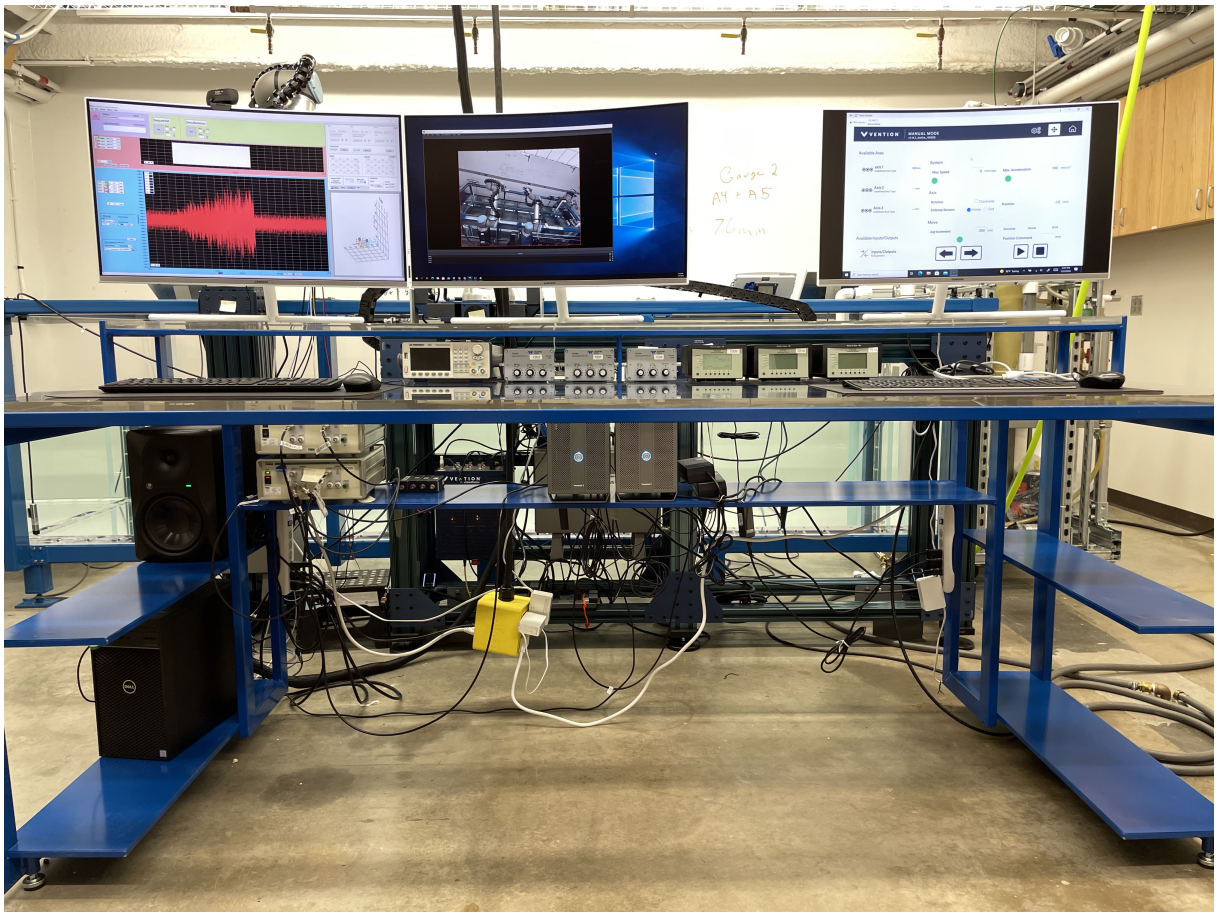

Figure 8: Computers and transducers used in the measurement chain. The ESAU interface is on the left screen; video feed from cameras in the lab are on the middle screen; and the interface for manual control of the Vention 7th axis-extender is on the right screen. Under the monitors but on top of the desk are the pre-amplifiers and signal conditioners. On the shelf below the desk, two TEGAM power amplifiers are on the left, next to the speaker, and the two chassis holding the Spectrum input and output cards are on the right.

transducers, including Digital to Analog (D-A) and Analog to Digital (A-D) components on the signal. The contribution of these components to the frequency response can ideally be accounted for by application of individual calibrated responses of each component of the measurement chain (shown in Fig. 8). Alternately, the contribution of all components may be accounted for by understanding the total through-the-sensor (TTS) response.[6,9,17–19] The technique for obtaining the TTS response relies on an *in situ* calibration to obtain the impulse response for the measurement system. This TTS response, $h_{\mathrm{TTS}}(t)$, can be obtained from the calibration measurement via the deconvolution method and then used as a filter (in deconvolution) on subsequent measurements to remove $h_{\mathrm{TTS}}(t)$ and obtain the impulse response, $h(t)$, corresponding to sound propagation in the water tank.[16]

The first step to obtaining the TTS response is taking a calibration measurement, where source and receiver are positioned close enough that transmission losses due to sound propagation are reduced significantly and reflections are easily removed. The small transmission losses during these calibration measurements are assumed negligible in this study; however, a phase adjustment accounting for the small propagation distance is applied. The small distance must be chosen with care and large compared to a wavelength for the frequency bandwidth of interest. Otherwise, potential near-field effects must be noted.

The calibration signal is a swept-sine signal, spanning the bandwidth of interest, which is broadcast and recorded. A chirp, spanning the frequencies of interest, is used as the calibration signal because long-duration swept-sine signals (chirps) provide the best signal-to-noise ratio for broadband measurements[6,10,16–18] compared with white noise, pulses,[20] or short swept-sine signals with averaging. This calibration measurement is interpreted through the deconvolution method (described below), and the resulting impulse response is time-gated for removal of all reflections in order to estimate the response of the measurement chain. This TTS calibration thus incorporates the unit-less sensitivities of all unknown components.[6,10,16] Application of this response to a subsequent measurement yields a calibrated measured response in Volts (which may be converted to μPa when a transducer sensitivity is applied in the preamplifier settings or directly to the data).

The impulse response obtained through frequency deconvolution[6,17,18] of the calibration measurement is time-gated using a half-Hanning window, with the time chosen to remove all reflections. The whole D-A and A-D measurement chain frequency response $H_{\mathrm{TTS}}(f)$ can then be obtained by applying a fast Fourier transform (FFT) on the windowed, time-gated response $h_{\mathrm{TTS}}(t)$.

After the TTS response $h_{\mathrm{TTS}}(t)$ is obtained from the calibration measurement, it can be applied to the received signal $r(t)$ to estimate the impulse response of the sound propagation in the environment, $h(t)$, may be found for subsequent measurements. For a generated signal, $g(t)$, the received signal, $r(t)$, is

$$r(t) = h(t) * h_{\mathrm{TTS}}(t) * g(t), \tag{1}$$

where h_{TTS} is the TTS response applied as a filter.[18] After a Fourier transform and rearranging, the frequency response (also referred to as the transfer function) associated with sound propagation in the tank is

$$H(f) = \frac{R(f)}{H_{\mathrm{TTS}}(f)G(f)}, \tag{2}$$

or by applying Wiener deconvolution to prevent division by zero:

$$H(f) = \frac{[H_{\mathrm{TTS}}(f)G(f)]^* R(f)}{[H_{\mathrm{TTS}}(f)G(f)]^2 + \sigma^2}. \tag{3}$$

An IFFT then yields the impulse response associated with the transfer function of the sound propagation independent of the frequency response of all the components in the measurement chain:

$$h(t) = \mathcal{F}^{-1}[H(f)]. \tag{4}$$

Thus, the frequency-dependent calibrated water-tank response can be obtained *in situ* for any source-receiver position under any propagation conditions. Since acoustic propagation models must adjust for varying conditions such as water temperature gradients,[2] this *in situ* calibration and measurement method provides the ability to obtain large data sets with full acoustic characterization.

4. LIMITATIONS AND IMPROVEMENTS

An open-air water tank of this size has numerous potential applications, however, limitations exist. The side walls, maximum depth and general dimensions limit the source-receiver range of potential scaled experiments.[3,9,10] Potential regimes for scaled experiments are also limited by the frequency response of the transducers. The size of transducers, mounts, etc. must be considered when designing the experiment as anything large relative to the wavelengths in the signals of interest have the potential to scatter the sound.

The selected attenuating material, the Apltile SF5048 panels, increases efficiency by reducing the reverberation time and, thus, the needed delay for repeatability between consecutive measurements. The panels,

however, are not 100% anechoic. Though other attenuating treatment options are available for different bandwidths,[3,5,9,10,13,20,21] passive underwater attenuating lining is often optimized for ultrasonic measurements and can be very costly. Multi-layered treatments, wider tanks, and active acoustic absorbers could improve the anechoic nature of the tank but also increase costs. Efforts to quantify the attenuating properties of the panel are ongoing.[11,22]

The positioning system utilizes UR10e robots to effectively scan the majority of the tank with any transducer orientation. A larger tank would allow for longer wavelengths and increased potential applications but require an even more creative solution to the positioning system[6,7] and larger lab space. The positioning could also be improved by having both robots on 7th axis extender tracks or even mounting the robots to a 7th axis extender gantry above the tank to fully reach any position in the tank. The robots also introduce electrical noise as mentioned above, and cabling requires a level of shielding that may be unnecessary with different systems or with lower desired bandwidths.

5. SUMMARY

An underwater acoustics research laboratory has been described with the goals of measuring large datasets efficiently for new research and helping students learn effective experimentation techniques. High priority has been given to measurement systems that are reliable, easy to use, and safe. Considerations that guided the design included the dimensions and materials of the tank, the capabilities of the data acquisition system, and the positioning systems precision. Underwater acoustic attenuating materials (such as the Apltile SF5048) are not likely to be truly anechoic, as defined in airborne anechoic chambers, but can significantly reduce reverberation time. Ultrasonic bandwidths require data acquisition systems that can handle high sampling rates, as well as care for dealing with potential sources of electrical noise in the cables. Robotic arms offer an alternative solution to traditional Cartesian positioning systems with high precision and variability in transducer orientation. Many transducers are available for tank measurements but require consideration of their physical size, as well as bandwidth and potential for needed impedance matching with amplification. To account for the frequency response of the measurement chain a through-the-sensor calibration method is employed. The combination of all of these tasks has opened the way for future underwater acoustics experiments at BYU.

6. ACKNOWLEDGEMENTS

We wish to acknowledge funding for the primary lab equipment from the Office Naval Research, Defense University Research Instrumentation Program N00014-18-S-F007, Grant 12671398.

REFERENCES

[1] C. T. Vongsawad, T. B. Neilsen, K. N. Terry, S. P. Hollingsworth, C. E. Dobbs, and G. H. Fronk, "Creating a mentored research environment in an underwater acoustics lab," The Journal of the Acoustical Society of America **150**(4), A292–A292 (2021) https://doi.org/10.1121/10.0008330 10.1121/10.0008330.

[2] L. T. Rauchenstein, A. Vishnu, X. Li, and Z. D. Deng, "Improving underwater localization accuracy with machine learning," Review of Scientific Instruments **89**(7) (2018) http://dx.doi.org/10.1063/1.5012687 10.1063/1.5012687.

[3] P. Papadakis, M. Taroudakis, F. Sturm, P. Sanchez, and J. P. Sessarego, "Scaled laboratory experiments of shallow water acoustic propagation: Calibration phase," Acta Acustica united with Acustica **94**(5), 676–684 (2008) 10.3813/AAA.918081.

[4] R. A. Hazelwood and S. P. Robinson, "Underwater acoustic power measurements in reverberant fields," in *Oceans 2007 - Europe*, IEEE, Aberdeen (2007), pp. 1–6, https://ieeexplore.ieee.org/document/4302295, 10.1109/OCEANSE.2007.4302295.

[5] D. C. Baumann, J. M. Brendly, D. B. Lafleur, P. L. Kelley, R. L. Hildebrand, and E. I. Sarda, "Techniques for Scaled Underwater Reverberation Measurements," in *Oceans 2019 MTS/IEEE SEATTLE*, IEEE, Seattle, WA, USA (2019), pp. 1–5, https://ieeexplore.ieee.org/document/8962732, 10.23919/OCEANS40490.2019.8962732.

[6] J. L. Kennedy, T. M. Marston, K. Lee, J. L. Lopes, and R. Lim, "A rail system for circular synthetic aperture sonar imaging and acoustic target strength measurements: Design/operation/preliminary results," Review of Scientific Instruments **85**(1) (2014) 10.1063/1.4861353.

[7] N. L. Weinberg and W. G. Grantham, "Development of an Underwater Acoustics Laboratory Course Development of an Underwater Acoustics Laboratory Course *," The Journal of the Acoustical Society of America **49**(3), 697–705 (1971) https://asa.scitation.org/doi/abs/10.1121/1.1912405 10.1121/1.1912405.

[8] L. Zhang and H. L. Swinney, "Sound propagation in a continuously stratified laboratory ocean model," The Journal of the Acoustical Society of America **141**(5), 3186–3189 (2017) http://dx.doi.org/10.1121/1.4983123 10.1121/1.4983123.

[9] J. D. Sagers, "Results from a scale model acoustic propagation experiment over a translationally invariant wedge," Proceedings of Meetings on Acoustics **22**(1) (2015) 10.1121/2.0000003.

[10] J. D. Sagers and M. S. Ballard, "Testing and verification of a scale-model acoustic propagation system," The Journal of the Acoustical Society of America **138**(6), 3576–3585 (2015) 10.1121/1.4936950.

[11] C. T. Vongsawad, "Development and characterization of an underwater acoustics laboratory via *in situ* impedance boundary measurements," Master's thesis, Brigham Young University (2021).

[12] C. B. Wallace and B. E. Anderson, "High-amplitude time reversal focusing of airborne ultrasound to generate a focused nonlinear difference frequency," The Journal of the Acoustical Society of America **150**(2), 1411–1423 (2021).

[13] Z. Deng, M. Weiland, T. Carlson, and M. Brad Eppard, "Design and instrumentation of a measurement and calibration system for an acoustic telemetry system," Sensors **10**(4), 3090–3099 (2010) 10.3390/s100403090.

[14] B. Van Damme, K. Van Den Abeele, Y. Li, and O. B. Matar, "Time reversed acoustics techniques for elastic imaging in reverberant and nonreverberant media: An experimental study of the chaotic cavity transducer concept," Journal of Applied Physics **109**(10) (2011) 10.1063/1.3590163.

[15] B. E. Anderson, M. Clemens, and M. L. Willardson, "The effect of transducer directivity on time reversal focusing," The Journal of the Acoustical Society of America **142**(1), EL95–EL101 (2017) http://dx.doi.org/10.1121/1.4994688 10.1121/1.4994688.

[16] K. L. Gemba and E.-M. Nosal, "Source characterization using recordings made in a reverberant underwater channel," Applied Acoustics **105**, 24–34 (2016).

[17] A. J. Berkhout, D. de Vries, and M. M. Boone, "A new method to acquire impulse responses in concert halls," Journal of the Acoustical Society of America **68**(1), 179–183 (1980) 10.1121/1.384618.

[18] A. Farina, "Advancements in impulse response measurements by sine sweeps," in *Audio Engineering Society - 122nd Audio Engineering Society Convention 2007*, May 2007, Audio Engineering Society, Vienna, Austria (2007).

[19] G. D. Curtis, "Wide-frequency response of type J-9 underwater sound projector in a typical experimental tank," Journal of the Acoustical Society of America **65**(3), 826–829 (1979) 10.1121/1.382504.

[20] P. R. Molina, J. S. Rebull, C. O. Anglés, and N. Ortega, "Method for the Acoustic Characterization of Underwater Sources in Anechoic Tanks Based on Simulated Free-Field Scenario," Instrumentation viewpoint; SIXTH INTERNATIONAL WORKSHOP ON MARINE TECHNOLOGY, Martech 2015 70–73 (2015) http://hdl.handle.net/2117/77608.

[21] V. G. Jayakumari, R. K. Shamsudeen, R. Ramesh, and T. Mukundan, "Modeling and validation of polyurethane based passive underwater acoustic absorber," The Journal of the Acoustical Society of America **130**(2), 724–730 (2011) 10.1121/1.3605670.

[22] C. E. Dobbs, G. H. Fronk, T. B. Neilsen, and C. T. Vongsawad, "Underwater acoustic intensity characterization of anechoic panels in laboratory tank," The Journal of the Acoustical Society of America **150**(4), A196–A196 (2021) https://doi.org/10.1121/10.0008109 10.1121/10.0008109.

[23] N. Cochard, J. L. Lacoume, P. Arzeliès, and Y. Gabillet, "Underwater Acoustic Noise Measurement in Test Tanks," IEEE Journal of Oceanic Engineering **25**(4), 516–522 (2000).